Comprehensive thermokinetic modelling and predictions of cellulose decomposition in isothermal, non-isothermal, and stepwise heating modes

Ahmed I. Osman [a, b*], Samer Fawzy [a], Charlie Farrell [c,d], Ala'a H. Al-Muhtaseb [e], John Harrison [c], Suhaib Al-Mawali [e], David W. Rooney [a]

[a] School of Chemistry and Chemical Engineering, Queen's University Belfast, Belfast BT9 5AG, Northern Ireland, UK

[b] Chemistry Department, Faculty of Science, South Valley University, Qena 83523 – Egypt.

[c] South West College, Cookstown, Co. Tyrone, BT80 8DN, Northern Ireland, UK.

[d] School of Mechanical and Aerospace Engineering, Queen's University Belfast, Belfast BT9 5AH, Northern Ireland, UK.

[e] Department of Petroleum and Chemical Engineering, College of Engineering, Sultan Qaboos University, Muscat, Oman.

Corresponding Authors: Ahmed I. Osman: (aosmanahmed01@qub.ac.uk), Ala'a H. Al-Muhtaseb (muhtaseb@squ.edu.om)

Address: School of Chemistry and Chemical Engineering, Queen's University Belfast, David Keir Building, Stranmillis Road, Belfast BT9 5AG, Northern Ireland, United Kingdom

Fax: +44 2890 97 4687

Tel.: +44 2890 97 4412

Abstract

The increasing significance of biomass in attaining ultimate sustainability in a multitude of vectors demands a deeper understanding of its underlying components. The pyrolytic breakdown of cellulose, a major biomass component, has been a subject of intense research since the 1950s, and despite significant research carried out and published thus far, the kinetics of cellulose degradation remains a source of debate. Herein, this work investigates the pyrolytic degradation of cellulose using Advanced Kinetics and Technology Solutions (AKTS) software. Kinetic parameters were computed using three methods, Friedman's differential iso-conversional, FWO and ASTM-E698. The results indicate E_a values of 40-181, 68-166, and 152.1 kJ/mol, using Friedman's, FWO and ASTM-E698 methods, respectively. Based on the results obtained via Friedman's differential iso-conversional method, predictions under isothermal, non-isothermal and stepwise heating profiles are presented. The predictions revealed that rapid degradation takes place up to 80% conversion, and a temperature of 350-400°C is required to efficiently achieve this, while temperatures of 650°C and higher are needed to efficiently achieve a 100% conversion in less than 2 hours.

Keywords:

Cellulose, Pyrolysis, Kinetic modelling, Thermokinetic predictions.

1.0 Introduction

Cellulose, an abundant biopolymer, is one of the major components of biomass, along with hemicellulose and lignin. As a natural polymer, cellulose is renewable, environmentally benign, low-cost, non–toxic, biodegradable, and biocompatible. Because of its hydrophilicity (ability to make hydrogen bonding), acid-insolubility, biocompatibility and biodegradability, microcrystalline cellulose as a type of cellulose has a wide range of applications in food, medicines, cosmetics, and other sectors [1]. Among cellulosic derivative products, cellulose acetate membranes have been widely utilised as nanofiltration, ultrafiltration and reverse osmosis membranes for water purification or dialysis treatment [2]. Other cellulose derivatives, such as cellulose ester and cellulose ether, have also been produced and marketed; the former is the most economically important, with several uses in the fibre, plastics, coatings, film and pharmaceutical sectors [3]. Different forms of pure cellulose (microcrystalline, low crystallinity or powdered) as well as its derivatives are used as excipients in the pharmaceutical industry in coat tablets, to control and/or sustain drug release, and improve powder mixture compressibility [4].

Cellulose typically consists of repeated β-D-glucopyranose units with 3-hydroxyl groups/anhydroglucose units, providing cellulose molecules with a high degree of functionality. Plants are currently the primary source of cellulose, which is found in plant cell walls; for instance, microcrystalline cellulose is extracted from cotton and woody cellulosic materials utilising dilute mineral acids (dil. HCl or dil. H_2SO_4).

The increasing significance of biomass in attaining ultimate sustainability in a multitude of vectors demands a deeper understanding of its underlying components. The pyrolytic breakdown of cellulose, in particular, has been a subject of intense research since the 1950s, and despite significant research carried out and published thus far, the kinetics of cellulose

degradation remains a source of debate [5,6]. Kinetic analysis facilitates the determination of the main parameters that describe the behaviour of the material being investigated under certain thermal conditions, namely apparent activation energy (E_a), rate of reaction and pre-exponential factor (k_0). The literature reports two main approaches in computing kinetic parameters, model-fitting and model-free methods[6-8]. Various kinetic studies on the pyrolytic conversion of cellulose have been carried out using these two methods[6]. It is worth noting that the international confederation for thermal analysis and calorimetry (ICTAC) kinetics committee has criticised model-fitting methods due to various computational drawbacks[8]. Model-free methods, on the other hand, provide a more robust computational platform for kinetic parameter determination. However, if mishandled may also lead to unreliable results[9]. The literature reports numerous model-free methods; however, the most prominent methods reported include Friedman's differential iso-conversional approach, the integral iso-conversional methods of Flynn-Wall-Ozawa (FWO) and Kissinger-Akahira-Sunrose (KAS) and the model-free non-isoconversional method ASTM-E698[6-8,10-12].

Several scholars have carried out the kinetic study of pyrolytic decomposition of cellulose using model-free methods. Capart et al. studied the thermal degradation of microgranular cellulose using Kissinger (also known as ASTM-E698) and Friedman's differential iso-conversional methods. The activation energy reported was 200 and ~136-203 kJ/mol using Kissinger and Friedman's models, respectively[13]. Sanchez-Jimenez et al. investigated commercial microcrystalline cellulose using Friedman's method and obtained an Ea value of approximately 190-192 kJ/mol throughout the conversion process, which declines to 119 kJ/mol towards the end of the reaction at ($\alpha = 0.9$)[14]. Hu et al. carried out the investigation using the FWO method and reported an average Ea value of 233 kJ/mol [15]. Dahiya et al. studied cellulose kinetics during pyrolysis using Friedman's, FWO and the modified Coats-Redfern methods obtaining Ea ranges of ~157-252, 159-168, and 157-166 kJ/mol between α

= 0.2-0.8, respectively[16]. Arora et al. reported Ea ranges of ~70-224, 133-175, and 132-175 kJ/mol using Friedman's, FWO and modified Coats-Redfern methods, respectively[17]. It is evident that the results reported in the literature are inconsistent. This may be due to various reasons, the type of cellulose and mass of sample used, as well as the heating rates and temperature range employed during experimentation[6].

With improvements in technology, kinetic modelling may now be done with extremely complex tools which facilitate advanced data optimisation options, computational precision, and the creation of reliable predictions. Herein, this work is the first to investigate the pyrolytic degradation of cellulose using Advanced Kinetics and Technology Solutions (AKTS) software. This advanced analytical software employs traditional thermo-analytical data to precisely compute the kinetic triplet using various model-free methods. Based on the highly robust kinetic results, the software is able to construct highly reliable predictions under various thermal profiles. AKTS has been successfully employed in many kinetic studies and is recognised as a reliable tool in conducting kinetic analysis [10,12,18-22]. The objective of this study is to present a holistic physicochemical investigation on cellulose and carry out a highly reliable kinetic study that strictly follows the ICTAC recommendations and, for the first time, report cellulose degradation predictions during pyrolysis under isothermal, non-isothermal and stepwise heating regimes.

2.0 Materials and methods

2.1 Materials and characterisation techniques

The cellulose material (microcrystalline) was purchased from Sigma Aldrich. The sample was used in powder form, with no further processing, for characterisation and kinetic modelling purposes. Furthermore, the sample was characterised using XRD, FTIR, TEM and XPS analyses, while elemental composition was determined using ultimate analysis. The supplementary material contains more information on the characterisation techniques.

2.2 Thermokinetic modelling and prediction methods

Kinetic modelling is typically used to better understand the thermal decomposition of various materials to obtain useful information about the reactions and the mechanisms involved. Various approaches discussed in the literature can be utilised in assessing the kinetic parameters, namely model-fitting and model-free methods. According to the ICTAC committee, model-free methods offer a higher degree of reliability and are prioritised for kinetic analysis compared to the model-fitting approach. Since the mechanisms behind cellulose degradation are complex, the model-free, differential iso-conversional technique, commonly known as the Friedman method, should be employed [23]. This is due to the advantages of not requiring any previous knowledge of the provided reaction mechanism, as well as the ability to evaluate the kinetic triplet across multiple conversion stages [10,24].

The theory behind the differential iso-conversional approach is detailed below:

As indicated in Equation 1 below, the rate of thermal degradation of a particular sample may be characterised in terms of the extent of conversion progress (α) and temperature (T).

$$\frac{d\alpha}{dt} = k(T)f(\alpha) \qquad \textit{Equation 1}$$

The degraded mass portion of cellulose is represented as in equation 2:

$$\alpha = \frac{m_i - m_a}{m_i - m_f} \qquad \textit{Equation 2}$$

where the initial, actual and final masses are m_i, m_u and m_f, respectively.

In addition, the Arrhenius equation (Equation 3) defines the temperature-dependent function in terms of activation energy and pre-exponential factor:

$$k(T) = k_o.e^{(-E_a/RT)} \qquad \textit{Equation 3}$$

where the rate constant is k, temperature is T in Kelvin, pre-exponential constant is k_o, activation energy is E_a and finally, the gas constant is R.

When equations 1 and 3 are combined, the equation for cellulose pyrolysis may be written as Equation 4 below.:

$$\frac{d\alpha}{dt} = k_o.e^{(-Ea/RT)} f(\alpha) \qquad \textit{Equation 4}$$

The sample is exposed to several constant linear heating rates that are designated as β in the non-isothermal isoconversional technique. Furthermore, it correlates to the temperature difference per unit time, as indicated in Equation 5 below:

$$\beta = \frac{dT}{dt} \qquad \textit{Equation 5}$$

The heating rate β in Equation 5 can then be applied to Equation 4 as shown below in Equation 6:

$$\frac{d\alpha}{dT} = \frac{k_o}{\beta}.e^{(-Ea/RT)} f(\alpha) \qquad \textit{Equation 6}$$

Finally, by substituting β using Equation 5 in Equation 6 and then applying the natural logarithm on both sides of Equation 6, the equation for Friedman's method is devised, allowing for the computation of E_a and k_o at different stages of reaction progress α

$$Ln\frac{d\alpha}{dt} = -\frac{E_a}{RT} + Ln[kof(\alpha)] \qquad \textit{Equation 7}$$

In addition to the differential iso-conversional method, various non-isothermal non-isoconversional (ASTM-E698) and isoconversional (FWO) methods, as presented below, are discussed in the literature and will be used for comparison purposes in this study.

ASTM-E698 method: This approach is more suited to describing single-step reactions, as presented in equation 8:

$$\beta\frac{d\alpha}{dT} = k_o \exp\left(-\frac{E_a}{RT}\right)(1-\alpha) \qquad \textit{Equation 8}$$

Flynn-Wall-Ozawa (FWO) method: This approach suggests utilising the integral iso-conversional analysis method to calculate changes in apparent activation energy in terms of distinct linear thermogravimetric curves; hence, it is quantitatively appropriate for multiple-step processes. The E_a may be determined by plotting the natural logarithm of heating rates (ln β) against 1000/T, yielding a linear relationship at different heating rates for a given conversion stage α, as shown in Equation 9.

$$\ln\beta = \ln\left(\frac{k_o.E_a}{R.g(\alpha)}\right) - 5.331 - 1.052\,\frac{E_a}{R.T} \qquad \textit{Equation 9}$$

where g(α) is constant at a given value of reaction progress (α).

In order to evaluate the kinetic parameters of cellulose pyrolysis, TGA experiments [25-28], using a Mettler Toledo Pyris TGA/DSC1, were carried out under an inert atmosphere (nitrogen flow was set at 40 cm^3/min), using five heating rates of 0.5, 1, 2, 4 and 8°C/min, allowing for a heating rate ratio of 16. It is worth noting that the TGA experiments were carried out in accordance with the ICTAC's guidelines for acquiring experimental thermal analysis data for kinetic calculations. This was done to provide accurate kinetic analysis results and excellent data resolution. Using the differential isoconversional approach, AKTS was used to calculate the kinetic triplet for cellulose pyrolysis. The software was also used to compare the activation energies determined using integral isoconversional (FWO) and non-isoconversional (ASTM E-698) methods.

The TGA values were then imported into AKTS software, and the DTG output was assessed using the program's derivation tool. After that, a horizontal baseline was built on each of the DTG signals to appropriately cover the sections of the DTG signals that varied from the flat baseline, showing pyrolysis and mass loss in each of the samples.

Assuming each DTG signal and corresponding created a baseline to be indicated by D(t) and B(t), respectively, the reaction rate and reaction progress can be calculated as shown below:

The reaction rate (RR):

$$\frac{d\alpha}{dt} = \frac{(D(t)-B(t))}{\int_{t_{initial}}^{t_{final}}(D(t)-B(t))dt} \qquad \textit{Equation 10}$$

Reaction progress (α):

$$\alpha(t) = \frac{\int_{t_{initial}}^{t}(D(t)-B(t))dt}{\int_{t_{initial}}^{t_{final}}(D(t)-B(t))dt} \qquad \textit{Equation 11}$$

After establishing baselines for all heating rates, a baseline optimisation exercise was run using 100 iterations to guarantee the R^2 value was as near to 1 as possible. Furthermore, the

optimisation would guarantee that the mass loss figures given for each heating rate were constant and did not have substantial variations owing to manual baseline formation. The data was then used to create a simulation, which was found to be a good match with some slight variations, most likely owing to instrument constraints. Following that, 100 iterations were performed to the simulated computations in order to guarantee precision and reproducibility. It is worth noting that AKTS generates high-resolution results covering 10,000 data points, which ensures model robustness. Finally, thermal predictions were made using AKTS, based on isothermal, non-isothermal, and stepwise heating configurations.

In this particular study, global lumped kinetic models were used in which cellulose pyrolysis is explained in sequences. However, there are other models, i.e., intrinsic reaction rate models, that consider the concentration of the reactants and products, which is considered as one of the elementary reaction models [29,30]. Due to the nature of microcrystalline cellulose pyrolysis and the lack of a dedicated reaction mechanism, we have opted to employ the differential isoconversional method, as it allows the computation of the kinetic triplet without requiring a defined reaction mechanism.

3.0 Results and discussion

3.1 **Characterisation results**

The XRD pattern of the microcrystalline cellulose is shown in Figure 1a, with diffractions at 2θ of 15.1º (101 plane), 22.8º (002) and 34.75º (004) corresponding to cellulose type I, where the diffraction lines that peak at 18.05 and 22.8º correspond to the amorphous and crystalline cellulose phases, respectively. The crystallinity index of the microcrystalline cellulose was determined using Eq.12, which is built on the greatest intensity obtained from the crystalline cellulose and the minimum point obtained from the amorphous cellulose phase [31].

$$\%\boldsymbol{CRI} = \frac{(\boldsymbol{I_{002}} - \boldsymbol{I_{am}})}{\boldsymbol{I_{002}}} \times \mathbf{100} \qquad \text{(Eq. 12)}$$

where I_{002} and I_{am} are the maximum intensity point of the crystalline peak at $2\theta = 22.6°$ and the minimum intensity point of the amorphous peak at $2\theta = 18.05°$

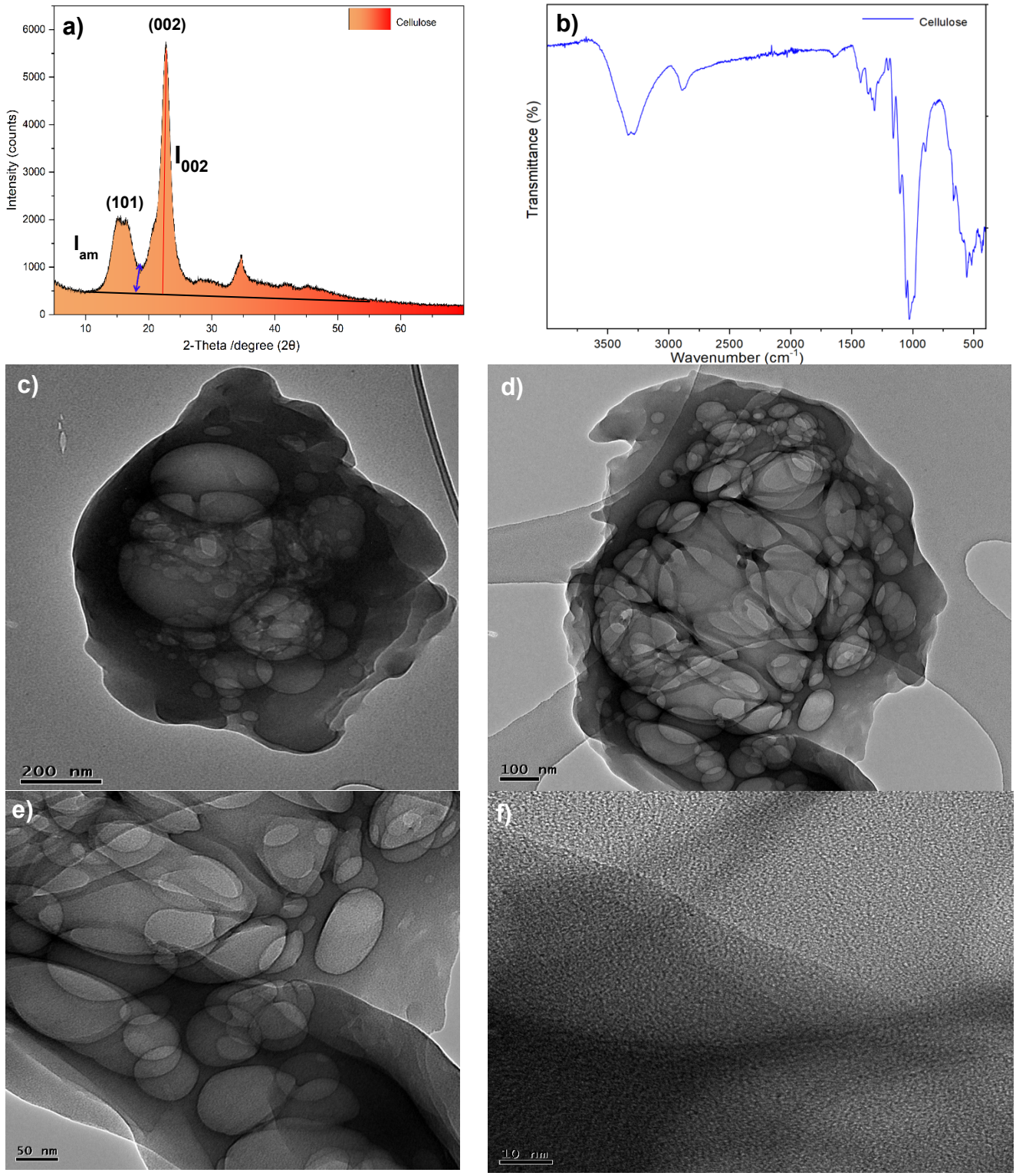

Figure 1: (a) XRD, (b) FTIR, and (c-f) TEM images of cellulose microcrystalline material.

It is not surprising that the crystallinity of cellulose herein is high at 83.3%, as the sample is in a microcrystalline phase. This is in line with the results of Herrera et al., reporting a %CRI of 85% for microcrystalline cellulose [32]. The variation in cellulose crystallinity results reported in the literature is attributed to the actual method used in analysis and the inherent characteristics of the material. Thygesen et al. reported %CRI in the range of 67-71% [33]. The FTIR of the microcrystalline cellulose material in the range of 500-4000 cm^{-1} is shown in Figure 1b. The characteristic bands of cellulose, C-H stretching (2890 cm^{-1}) and C-O stretching (range of 1050-1150 cm^{-1}) are observed in Figure 1b, which are attributed to the bonding in the polysaccharide aromatic rings [34]. The absorption bands observed at 1060 and 1380 cm^{-1} are attributed to the C-O-C bond in the pyranose ring in the cellulose structure and microcrystalline cellulose presence, respectively. Finally, the glycosidic bonding between the sugar components within the cellulose is represented by the absorption band at 900 cm^{-1} [35]. The hydrophilicity of the microcrystalline cellulose was confirmed by the O − H stretching broad absorption band at approximately 3400 cm^{-1}.

The TEM was used to observe the morphology of the cellulose material, as shown in Figure 1 c-f, with a spherical-like structure. It has been reported that the morphology and shape structure of cellulose vary significantly depending on the precursor and preparation method [36,37]. According to previous research, the size and shape of nano cellulose impact their characteristics (for example, optical capabilities, stability, and rheology) in aqueous media, which greatly influences their use. Cellulose with a spherical or square shape is ideal as a Pickering emulsion stabiliser or drug delivery carrier for encapsulation [38,39]. A particle size range from 15.0-34.6 nm is observed.

To better understand the surface property of the cellulose material used in this study, XPS analysis was performed. Figure 2a depicts the survey spectra of microcrystalline cellulose; aside from the typical elements in cellulose, such as carbon (C *1s* at 284.7 eV) and oxygen (O

1s at 531.6 eV), no other contaminants were found [40]. High-resolution *C 1s* peaks appeared at binding energies of approximately 284.5, 287.1 and 288.5 eV, which are attributed to C=C or C-C, C=O and O-C=O bonding, respectively (Figure 2b) [41], while the O *1s* spectra showed C=O oxygen species, as shown in Figure 2c. The CHNS analysis showed that the wt.% of C, H, N and S were 43.68, 6.65, 0.70 and 0.62%, respectively. The results are in line with the literature reported on cellulose (microcrystalline type) [42,43].

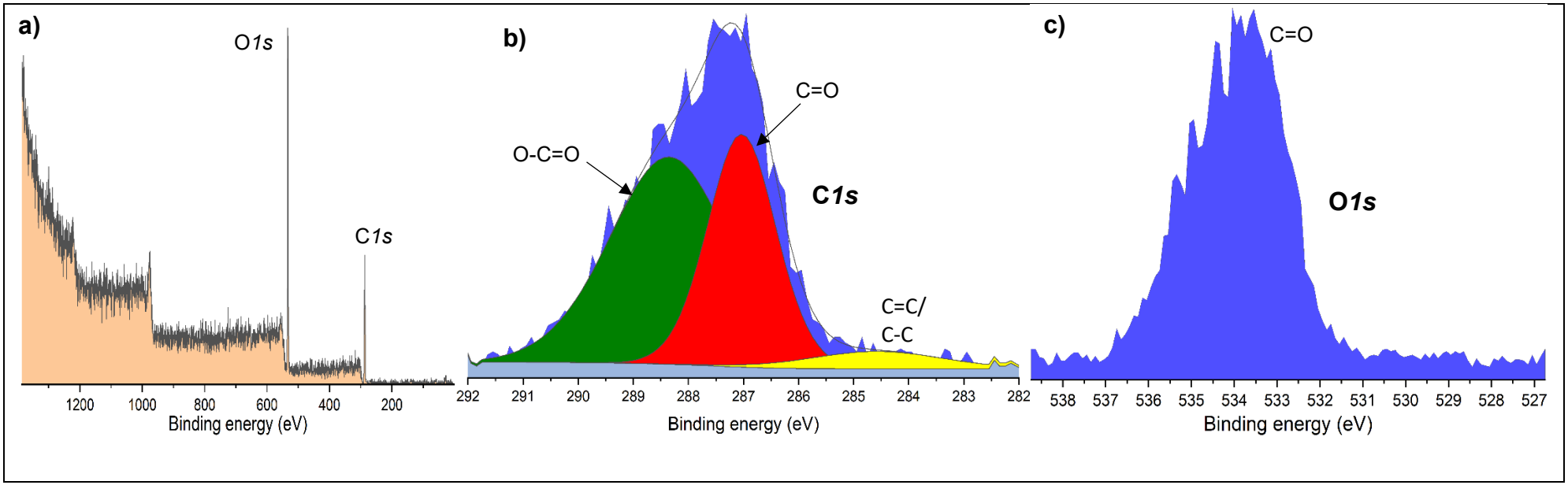

Figure 2: (a) XPS survey spectra, (b) High-resolution *C 1s* peaks, and (c) High-resolution *O 1s* peaks of microcrystalline cellulose material.

3.2 Kinetic modelling results

Non-isothermal thermogravimetric analysis was carried out in an inert environment at five different heating rates of 0.5, 1, 2, 4, and 8°C/min. It is worth noting that the ratio between the slowest and fastest heating rates is 16, meeting the ICTAC recommendations, which necessitate at least a ratio of 10-15 between fastest and slowest heating rates for a high level of precision[44]. Figure 3 presents the results of the five heating rates, showing mass loss as a function of temperature. It can be observed that that the reaction proceeds in three stages. A gradual decline can be observed during the initial stage until 270-300°C, and this is usually due to dehydration along with the initial decomposition stage. This is followed by a very sharp curve, where most of the cellulosic decomposition takes place. Based on the heating rate, this second stage occurs between 270-300°C and 310-370°C. Almost 80% mass loss is detected in this stage. However, cellulose continues to degrade after 370°C, the third stage, at a very slow rate. The results are consistent with cellulose TGA findings reported in the literature[45,46].

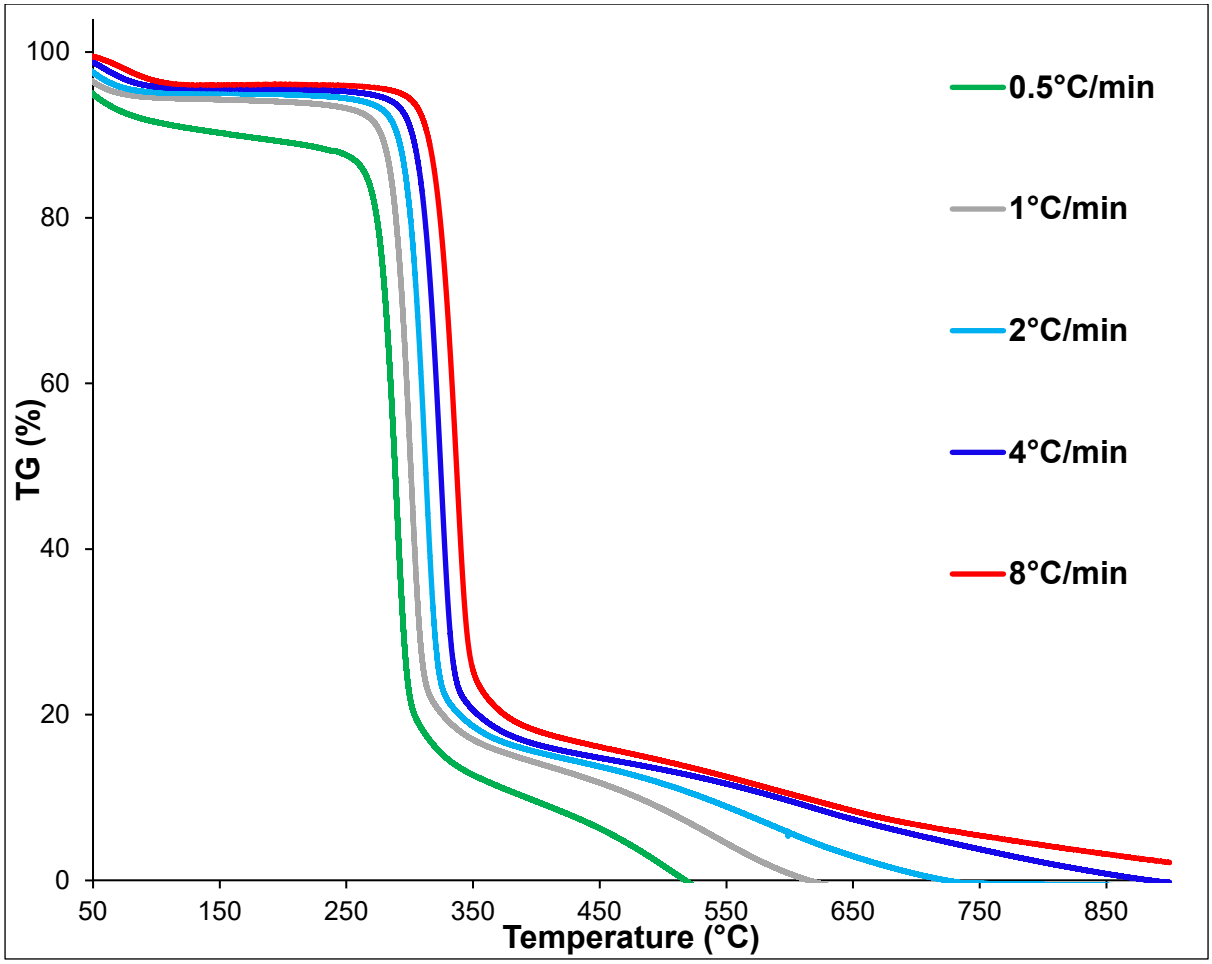

Figure 3: TGA results for cellulose pyrolysis at heating rates of 0.5, 1, 2, 4 and 8°C/min.

Based on the TGA data, AKTS software was used to determine the kinetic triplet using Friedman's differential iso-conversional method. For comparison purposes, the FWO integral iso-conversional approach and ASTM-E698 model-free non-isoconversional technique were also used. Figure 4a depicts the reaction progress under the five heating rates. As noted, the simulated and actual results are highly correlated with an R^2 value of 0.9783. As the heating rate increases, a shift in reaction temperature is noted, which is mainly explained by thermal lag. Figure 4b presents the reaction rate of cellulose pyrolysis based on the five heating rates. Once again, the simulated and actual results are highly correlated. Maximum reaction rates of 0.000295, 0.000568, 0.001108, 0.002161 and 0.004088 1/s are observed at temperatures of

290, 300, 312, 325 and 337°C for the 5 heating rates, respectively. Approximately a 14-fold increase in reaction rate is observed between the slowest and fastest heating rates.

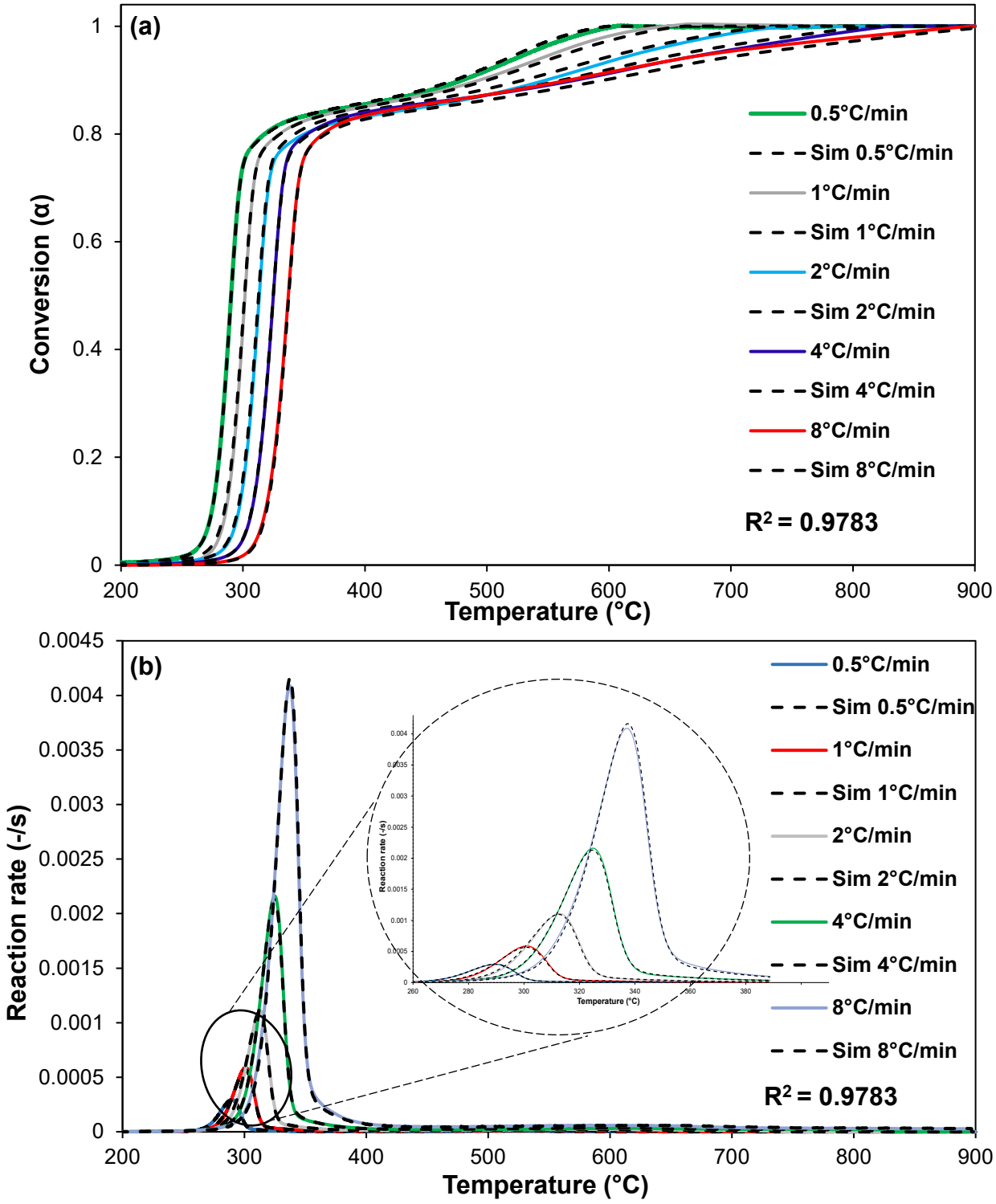

Figure 4: (a) reaction progress and (b) reaction rate as a function of temperature at various heating rates.

Figure 5a presents the apparent activation energy computed via the ASTM-E698 method, where the results indicate an E_a value of 152.1 kJ/mol. This method is well suited to single-step reactions and may be inadequate to describe cellulose decomposition, considering the nature of the primary and secondary reactions involved in cellulose decomposition. Figure 5b, depicts the results of the FWO method where the natural logarithm of heating rate is plotted against inverse temperature. As noted, the results are well-matched, and the trend lines are consistent. Figure 5c presents the activation energy for cellulose pyrolysis as the reaction advances. As indicated, a sharp increase in E_a is observed during the initial stage of the conversion, reaching ~161 kJ/mol at α=0.05. The E_a value remains around this value (161-162 kJ/mol) between α= 0.05 – 0.7 and then slightly increases to ~ 166 kJ/mol at α= 0.8. Furthermore, a decline is noted until an E_a value of 68 kJ/mol is reached towards the end of the conversion. The results obtained are highly consistent with the FWO results reported by Dahiya et al. of 159-168 kJ/mol between α=0.2 - 0.8[16]. Although we have already mentioned the inadequacy of the ASTM-E698 method, it is still worth noting that the E_a value obtained is similar to the average value observed during most of the conversion process via FWO.

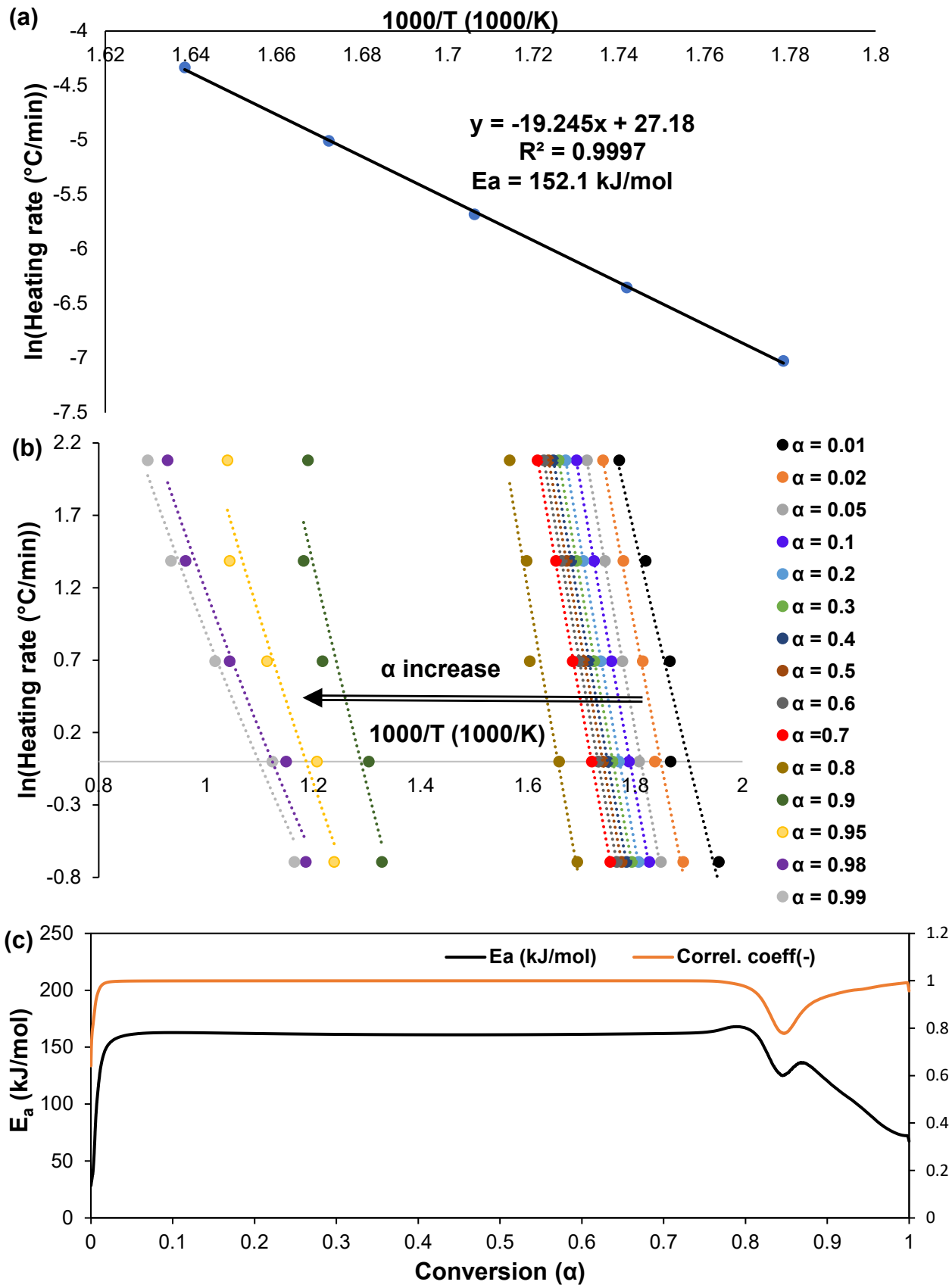

Figure 5: (a) apparent activation energy (Ea) results via ASTM-E698 method, and (b,c) kinetic results obtained via FWO method.

The results computed via Friedman's differential iso-conversional method are depicted in Figure 6a, plotting the natural logarithm of reaction rate against inverse temperature and Figure 6b, presenting the apparent activation energy (E_a) and pre-exponential factor (k_0) as the conversion advances. A sharp rise is observed initially reaching an E_a value of ~187 kJ/mol at α=0.014, decreasing to 157 kJ/mol at α=0.2. The E_a then exhibits a very slow rise over the course of the reaction from α=0.2 - 0.75, where an increase from 157 to 168 kJ/mol is noted. A sudden spike is noted between α=0.75 and 0.77, with E_a reaching 181 kJ/mol and then starts to decrease, reaching ~40 kJ/mol towards the end of the conversion. The results are very comparable to those obtained via FWO, especially between α=0.2 - 0.75. Table 1 presents the E_a findings obtained in this study as well as the ones reported in the literature. As previously suggested, the differences observed can be due to various reasons, which include inherent characteristics of the type of cellulose used, differences in sample weight utilised for experimentation, the choice of different heating rates and different temperature ranges. However, following the ICTAC's recommendation and using a highly sophisticated tool, the results presented for this specific cellulose sample are robust and can be used for constructing reliable degradation predictions under various heating regimes.

Table1: Kinetic results for cellulose pyrolysis obtained in this study using Friedman's and FWO methods compared to the literature.

α	This Study				Dhaiya et al. (2008)				Sanchez-Jimenez et al.		Capart et al. (2004)		Arora et al. (2011)			
%	Differential Iso-Conversional		FWO		Differential Iso-Conversional		FWO		Differential Iso-Conversional		Differential Iso-Conversional		Differential Iso-Conversional		FWO	
	kJ/mol	*Correlation*	*kJ/mol*	*Correlation*	*kJ/mol*	*Correlation*	*kJ/mol*	*Correlation*	*kJ/mol*	*Correlation*	*kJ/mol*	*Correlation*	*kJ/mol*	*Correlation*	*kJ/mol*	*Correlation*
5	166.78	0.9992	161.27	0.9989	-	-	-	-	-	-	-	-	-	-	-	-
10	161.59	0.9998	162.81	0.9995	-	-	-	-	191 +/- 6	0.997	200	-	148.1	-	167.8	-
15	158.68	0.9999	162.5	0.9997	-	-	-	-	-	-	-	-	168.5	-	162.5	-
20	157.42	0.9999	162.02	0.9998	159.8	0.9783	158.9	0.9964	192 +/- 4	0.998	199	-	179.1	-	161.3	-
25	157.43	0.9999	161.6	0.9998	-	-	-	-	-	-	-	-	156.8	-	160.9	-
30	156.95	0.9999	161.27	0.9998	169.8	0.9985	162.7	0.9995	192 +/- 4	0.999	202.4	-	152.1	-	158	-
35	157.96	0.9999	161.05	0.9999	-	-	-	-	-	-	-	-	148.7	-	157.6	-
40	158.73	0.9999	160.93	0.9999	160.6	0.9479	164	0.9999	192 +/- 4	0.999	199.6	-	134.1	-	156.5	-
45	159.55	0.9999	160.88	0.9999	-	-	-	-	-	-	-	-	132.6	-	155.5	-
50	160.52	0.9999	160.93	0.9999	175.6	0.9936	165.2	1	191 +/- 4	0.999	201.9	-	135.5	-	154.3	-
55	161.76	0.9998	161.06	0.9999	-	-	-	-	-	-	-	-	139.8	-	152.9	-
60	162.5	0.9997	161.29	0.9999	162.5	0.9993	164.6	1	190 +/- 4	0.999	202.6	-	141.7	-	151.9	-
65	163.45	0.9993	161.6	0.9999	-	-	-	-	-	-	-	-	140.8	-	150.8	-
70	163.78	0.9979	162	0.9998	157.2	0.979	164.6	1	190 +/- 4	0.999	192.9	-	140.2	-	150.6	-
75	171.22	0.984	163.08	0.9993	-	-	-	-	-	-	-	-	146.6	-	156.3	-
80	164.94	0.92807	166.83	0.9754	251.9	0.9433	168.1	1	190 +/- 4	0.999	136.21	-	147.9	-	149	-
85	113.51	0.7577	126.59	0.7816	-	-	-	-	-	-	-	-	100.2	-	134.2	-
90	98.62	0.9118	120.37	0.9345	-	-	-	-	119 +/- 32	0.831	-	-	69.7	-	132.8	-
95	54.05	0.9585	91.72	0.9686	-	-	-	-	-	-	-	-	-	-	-	-
99	41.04	0.9948	67.37	0.9891	-	-	-	-	-	-	-	-	-	-	-	-
Type:	Microcrystalline cellulose powder - Sigma AlDrich				Cellulose powder - CDH (India)				Microcrystalline cellulose -		Microcrystalline cellulose		Microcrystalline cellulose - Acros Organics (USA)			
Heating Rate:	0.5, 1, 2, 4, 8°C/min				2, 5, 10°C/min				1, 2, 5, 10°C/min		1.05, 2.1, 3.2, 6.5, 10.9°C/min		2.5, 5, 10, 20°C/min			
Temperature:	Ambient - 900°C				Ambient - 700°C				-		Ambient - 700°C		Ambient - 700°C			
Sample weight:	20mg				6 - 8 mg				8 - 10 mg		4 - 7 mg		3 - 6 mg			

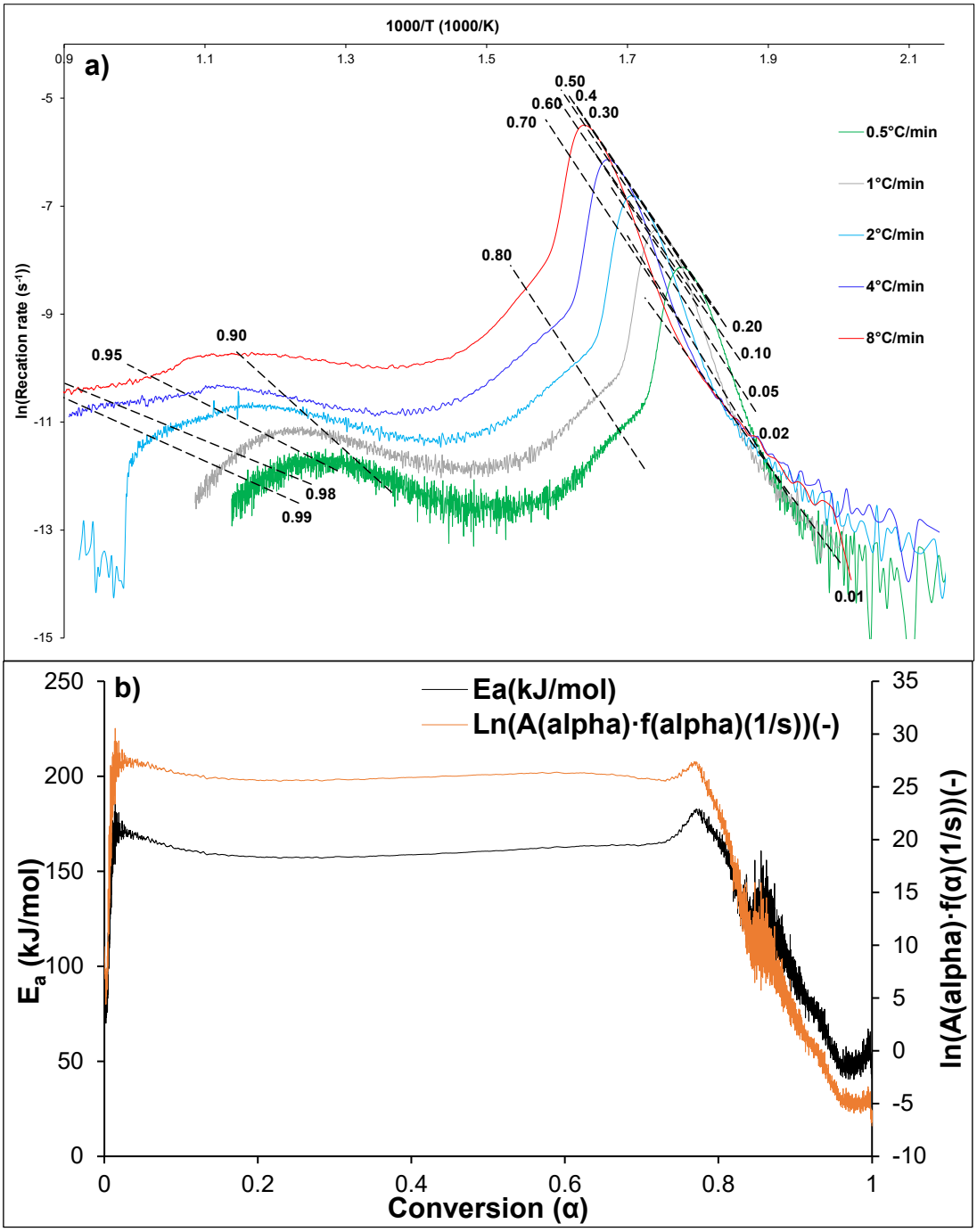

Figure 6: Kinetic parameters for cellulose pyrolysis using Friedman's method (a,b).

3.3 Thermal predictions of cellulose pyrolysis

Predictions for Isothermal, non-isothermal and step-based heating modes, representing various types of reactors, are constructed via AKTS using the results obtained through Friedman's method. The predictions facilitate a better understanding of cellulose behaviour under different heating modes. Figure 7 presents cellulose pyrolysis predictions under isothermal conditions. The temperature range was set at 250 - 800°C, in increments of 50°C. It can be noted that the reaction reaches completion in approximately 35 minutes at 800°C. At lower temperatures, completion is achieved within 47 to 246,039 minutes, based on 750 to 250°C, respectively. Furthermore, it can be observed that approximately 80% conversion is reached in less than 0.125 minutes at 450°C and higher temperatures. At such temperatures, rapid decomposition occurs almost immediately and then continues gradually until the reaction is complete. At 400°C rapid decomposition is also observed, and an 80% conversion is achieved within 0.7 minutes. At 300 and 350°C, 80% conversion is achieved within 107 and 6.56 minutes, respectively. For temperatures below this range, conversion is extremely slow. Table 2 presents the predicted time taken to reach various conversion stages until the end of the conversion process. The values highlighted in red indicate impractical time taken, while values highlighted in green indicate time below 2 hours, which is highly recommended from an efficiency point of view. The values highlighted in grey indicate practical yet inefficient process timing. The results indicate that pyrolysis at 250°C is very inefficient and reaching a complete conversion is impractical. A complete conversion can be practically reached, yet inefficiently at a temperature range of 450-600°C, while at 650°C and above, practical and efficient results can be obtained. To reach a 90% conversion, practical and efficient conversion can be reached at 450°C in a total processing time of approximately 2 hours. Higher temperatures significantly accelerate the conversion process, where a 90% conversion can be achieved between 0.39 –

38.7 minutes, based on a temperature range of 500-800°C, where the shorter time is associated with the highest processing temperature.

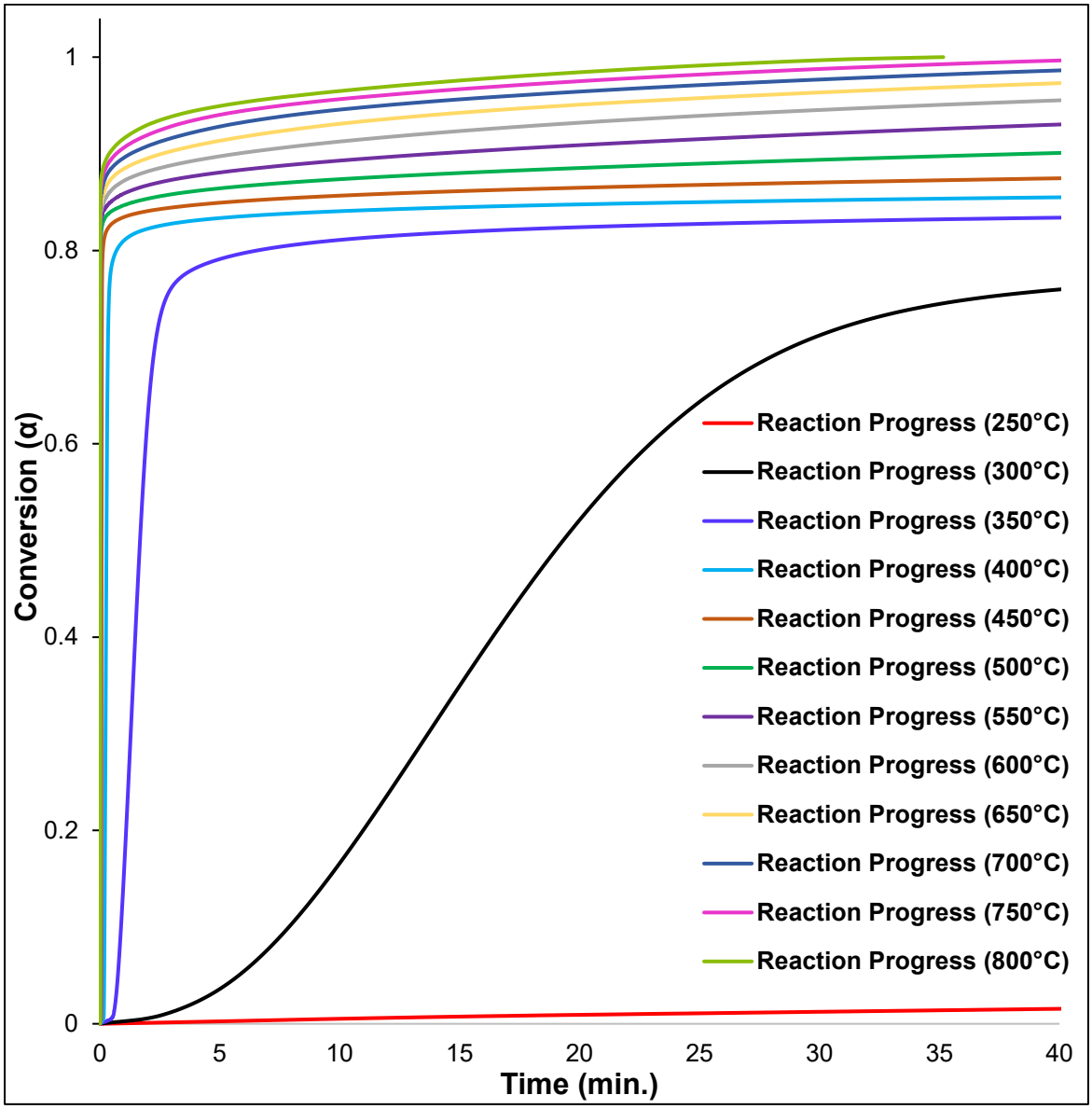

Figure 7: Isothermal predictions for pyrolytic conversion of cellulose at a temperature range of 250-800°C.

Table2: Time is taken to reach various conversion stages at a temperature range of 250-800°C, based on isothermal heating.

α %	10	20	30	40	50	60	70	80	90	100
Temp (°C)	**minutes**									
250	170	245	308	374	445	538	695	3235	197864	246039
300	7.88	11	13.68	16.42	19.33	22.95	28.88	107.5	17914	29389
350	0.88	1.1	1.29	1.48	1.68	1.91	2.29	6.58	2532	6250
400	0.193	0.215	0.235	0.255	0.275	0.298	0.335	0.697	497	1999
450	0.062	0.065	0.068	0.071	0.074	0.077	0.082	0.125	126	837
500	0.0249	0.0255	0.026	0.0265	0.027	0.0276	0.0284	0.0352	38.7	418
550	0.01143	0.011557	0.011676	0.011792	0.011903	0.012024	0.012201	0.013551	13.9	235
600	0.005811	0.005844	0.005875	0.005906	0.005936	0.005967	0.006012	0.006334	5.7	145
650	0.003198	0.003208	0.003218	0.003227	0.003236	0.003246	0.003259	0.003349	2.58	95
700	0.001878	0.001882	0.001885	0.001888	0.001892	0.001895	0.001899	0.001928	1.28	65
750	0.001165	0.001166	0.001167	0.001169	0.00117	0.001171	0.001173	0.001183	0.68	47
800	0.000756	0.000757	0.000757	0.000758	0.000759	0.000759	0.00076	0.000764	0.39	35

Figure 8 depicts the prediction results under non-isothermal conditions using 10, 20, 30, 40 and 50°C/min heating rates. As noted, to reach an 80% conversion at a temperature range of 380- 410°C is required, based on the range of heating rates used, 10-50°C/min, respectively. However, this gap widens towards the end of the conversion process. To reach a complete conversion, this is achieved at 964, 1096, 1187, 1258 and 1318°C, within 93, 53, 39, 31 and 26 minutes at heating rates of 10, 20, 30, 40 and 50°C/min, respectively. The results clearly indicate that most cellulose degradation occurs at around 400°C, irrespective of the heating rate used.

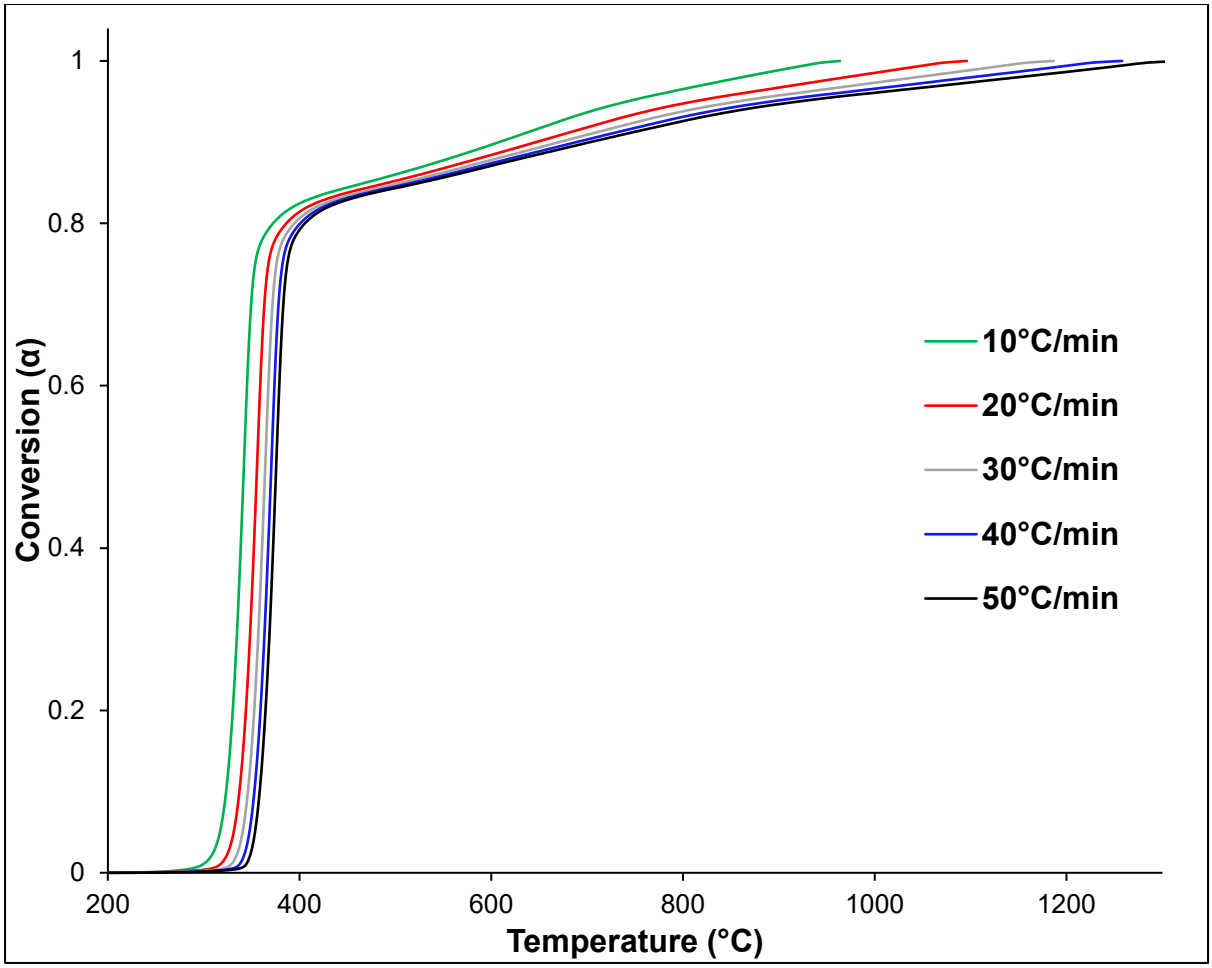

Figure 8: Non-isothermal prediction results for pyrolytic conversion of cellulose-based on heating rates of 10, 20, 30, 40 and 50°C/min.

Figure 9a-f presents the stepwise heating prediction results for six scenarios where ramped heating is carried out at 10°C/min followed by a temperature hold for 8 hours at temperatures between 300 - 800°C. These heating profiles represent batch type reactors where the material undergoes a heat ramp from ambient, followed by a hold period at a specified temperature. The results once again suggest rapid degradation during the initial stage of conversion, followed by gradual decomposition. This trend is observed across all holding temperatures. For a 10°C/min ramp and a holding temperature of 300°C (Figure 9a), it can be noted that approximately 80% conversion is achieved after 132 minutes, where most of the decomposition took place starting from minute 28 until minute 132 after reaction initiation. A maximum reaction rate of 0.000628 1/s is observed at 39 minutes from the start of the reaction, which is achieved at 32%

conversion. It is worth noting that the holding period of 8 hours is not sufficient to complete the reaction, where only 83% conversion is reached. For all other holding temperatures (Figure 9b-f), the initial rapid degradation phase is observed between minutes 28 and 35, where approximately 80% of the conversion is achieved. This stage takes place between 300 and 372°C, where a maximum reaction rate of 0.005174 1/s is noted at 341°C, ~ 32 minutes after reaction initiation, corresponding to ~ 50% conversion. For a temperature of 400°C, the holding period of 8 hours is still not yet sufficient, where only 90% of the reaction is completed. A complete reaction is achieved at 461, 197, 126, and 102 minutes for temperatures of 500, 600, 700, and 800°C, respectively.

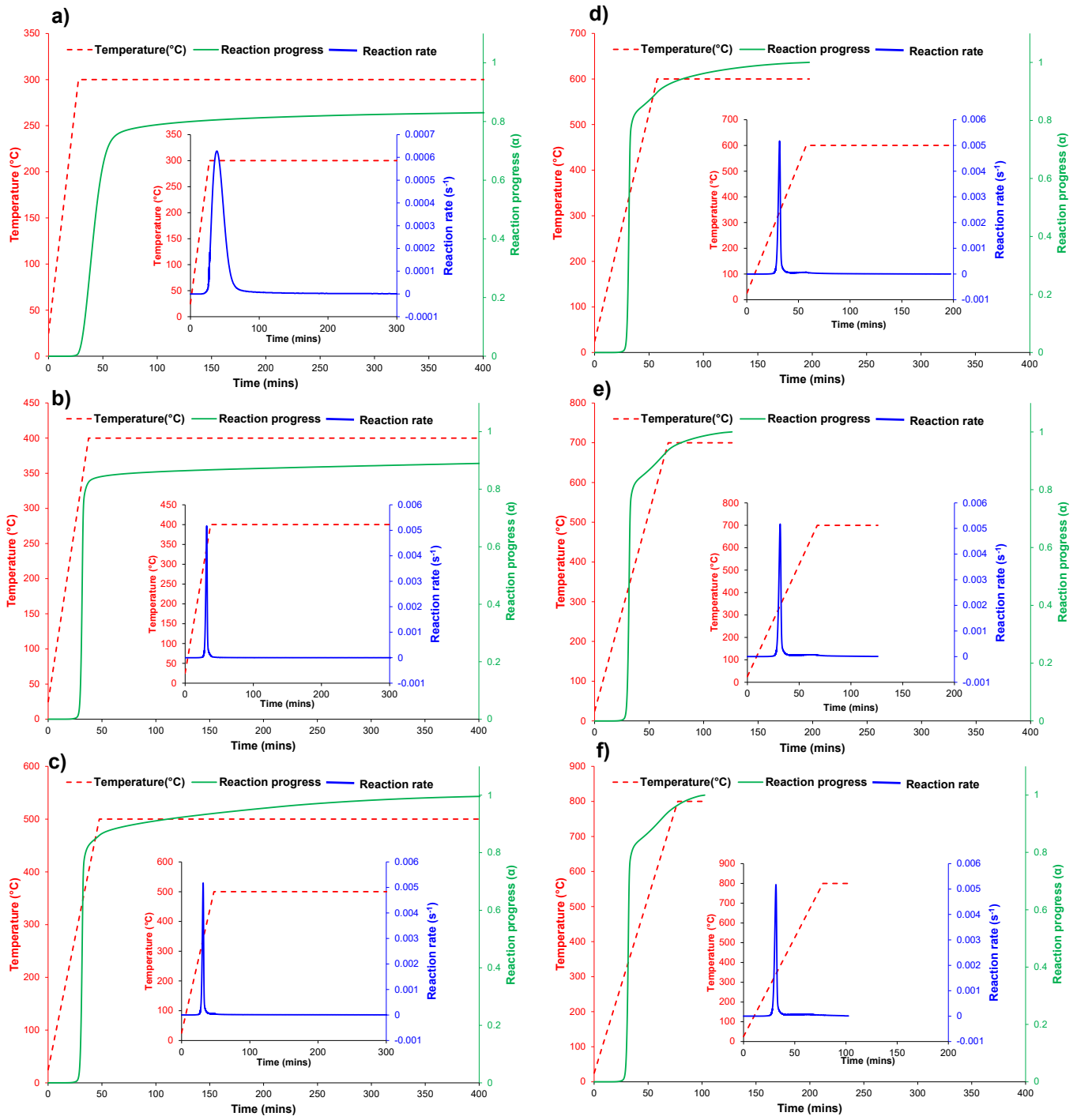

Figure 9: Stepwise prediction results for pyrolytic conversion of cellulose using a temperature ramp of 10°C/min and final holding temperature of 300-800°C (a-f).

Figure 10a-d presents the stepwise predictions for four scenarios using heating rates of 5, 10, 20 and 50°C/min for temperature ramping, followed by a holding period of 8 hours at a temperature of 500°C. Once again, rapid decomposition is observed during the initial phase, up to 80% conversion. The impact of heating rate is clearly noted, where 80% conversion occurs between minute 52 – 66, 28 – 35, 14.5 – 18, and 6 – 8, from reaction initiation, using heating rates of 5, 10, 20 and 50°C/min, respectively. Additionally, the reaction reaches completion within 505, 461, 440 and 426 minutes for the same order of heating rates presented.

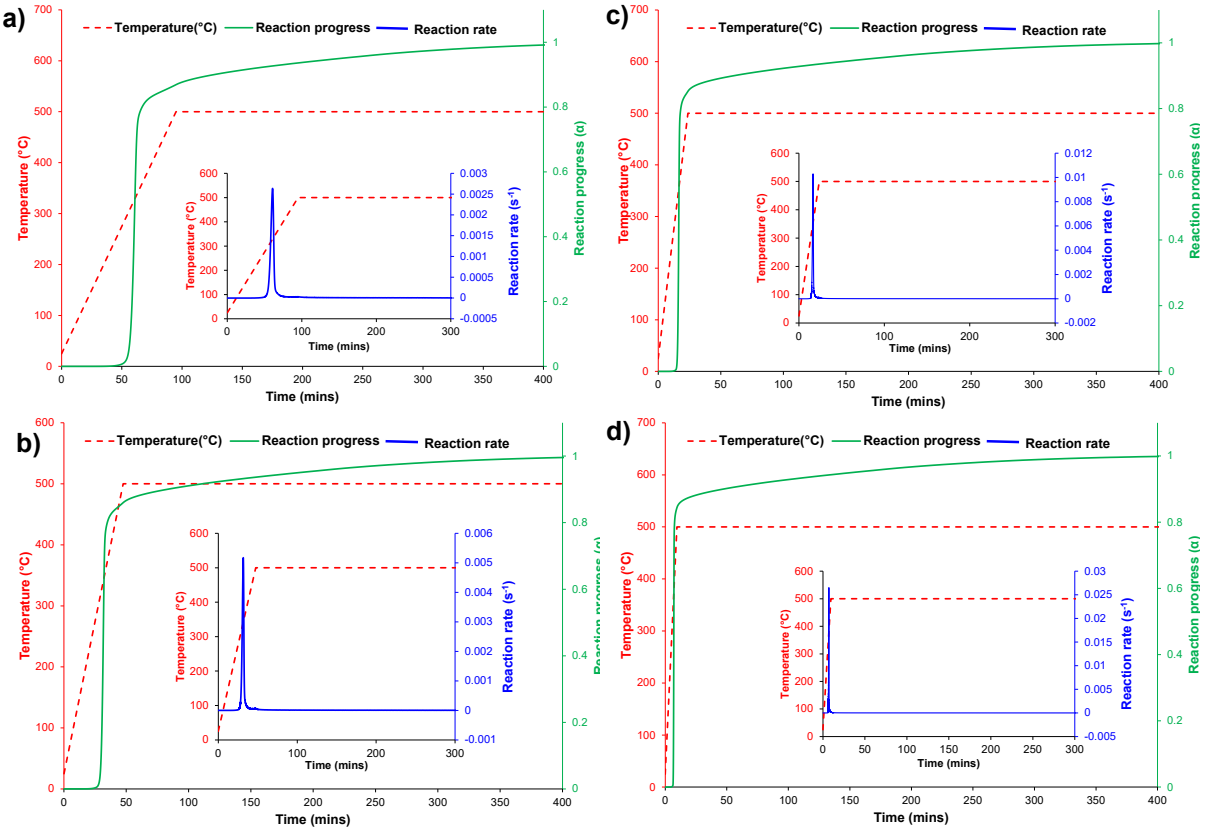

Figure 10: Stepwise prediction results for pyrolytic conversion of cellulose using various temperature ramps of 5,10, 20 and 50°C/min and final holding temperature of 500°C (a-d).

4.0 Conclusion

This study carried out an investigation on the kinetic behaviour of microcrystalline cellulose during pyrolysis. Firstly, the physicochemical properties of the material were evaluated. Furthermore, AKTS was utilised to determine the kinetic parameters and make predictions under different thermal settings. Kinetic parameters were computed using three methods, Friedman's differential iso-conversional, FWO and ASTM-E698. The results indicate an E_a value of 40-181, 68 -166, and 152.1 kJ/mol, using Friedman's, FWO and ASTM-E698 methods, respectively. It is worth noting that the results obtained via Friedman's and FWO are, to a certain extent, consistent with the literature. Isothermal, non-isothermal, and stepwise predictions, representing different types of reactors, were generated based on the results derived using the differential iso-conversional method. The predictions revealed that rapid degradation takes place up to 80% conversion, and a temperature of 350-400°C is required to efficiently achieve this, while temperatures of 650°C and higher are needed to efficiently achieve a 100% conversion that is in a period under 2 hours. More experimental research is required to confirm the findings of this study.

Credit Author Statement

Ahmed I. Osman: Conceptualization, Methodology: Ahmed I. Osman, Samer Fawzy, Charlie Farrell, Suhaib Al-Mawali and Ala'a H. Al-Muhtaseb. Writing- Original draft preparation. Ahmed I. Osman and Samer Fawzy. Writing- Reviewing, Supervision and Editing, John Harrison, and David W. Rooney.

Acknowledgement

The authors wish to acknowledge the support of The Bryden Centre project (Project ID VA5048). The Bryden Centre project is supported by the European Union's INTERREG VA Programme, managed by the Special EU Programmes Body (SEUPB).

Disclaimer:

The views and opinions expressed in this paper do not necessarily reflect those of the European Commission or the Special EU Programmes Body (SEUPB).

Conflict of interest

The authors declare that no conflict of interest.

5.0 References:

[1] M. Bushell, J. Meija, M. Chen, W. Batchelor, C. Browne, J.-Y. Cho, C.A. Clifford, Z. Al-Rekabi, O.M. Vanderfleet, E.D. Cranston, M. Lawn, V.A. Coleman, G. Nyström, M. Arcari, R. Mezzenga, B.C. Park, C. Shin, L. Ren, T. Bu, T. Saito, Y. Kaku, R. Wagner and L.J. Johnston, *Cellulose*, 28, (2021) 1387.

[2] M. Shimizu, R. Álvarez-Asencio, N. Nordgren and A. Uedono, *Cellulose*, 27, (2019) 1357.

[3] P. Xiao, J. Zhang, Y. Feng, J. Wu, J. He and J. Zhang, *Cellulose*, 21, (2014) 2369.

[4] S.M.A.S. Keshk, A.A. El-Zahhar, Q.A. Alsulami, M. Jaremko, S. Bondock and T. Heinze, *Cellulose*, 27, (2019) 1603.

[5] A. Paajanen, A. Rinta-Paavola and J. Vaari, *Cellulose*, 28, (2021) 8987.

[6] C. Şerbănescu, *Chemical Papers*, 68, (2014) 847.

[7] R.K. Mishra and K. Mohanty, *Bioresource Technology*, 251, (2018) 63.

[8] L. Luo, X. Guo, Z. Zhang, M. Chai, M.M. Rahman, X. Zhang and J. Cai, *Energy & Fuels*, 34, (2020) 4874.

[9] S. Vyazovkin, A.K. Burnham, J.M. Criado, L.A. Pérez-Maqueda, C. Popescu and N. Sbirrazzuoli, *Thermochimica Acta*, 520, (2011) 1.

[10] A.I. Osman, C. Farrell, A.H. Al-Muhtaseb, A.S. Al-Fatesh, J. Harrison and D.W. Rooney, *Environmental Sciences Europe*, 32, (2020) 112.

[11] J. Bonilla, R.P. Salazar and M. Mayorga, *Heliyon*, 5, (2019) e02723.

[12] C.I. Akor, A.I. Osman, C. Farrell, C.S. McCallum, W. John Doran, K. Morgan, J. Harrison, P.J. Walsh and G.N. Sheldrake, *Chemical Engineering Journal*, 406, (2021) 127039.

[13] R. Capart, L. Khezami and A. Burnham, *Thermochimica Acta*, 417, (2004) 79.

[14] P.E. Sánchez-Jiménez, L.A. Pérez-Maqueda, A. Perejón, J. Pascual-Cosp, M. Benítez-Guerrero and J.M. Criado, *Cellulose*, 18, (2011) 1487.

[15] S. Hu, A. Jess and M. Xu, *Fuel*, 86, (2007) 2778.
[16] J.B. Dahiya, K. Kumar, M. Muller-Hagedorn and H. Bockhorn, *Polymer International*, 57, (2008) 722.
[17] S. Arora, S. Lala, S. Kumar, M. Kumar and M. Kumar, *Archives of Applied Science Research*, 3, (2011) 188.
[18] S. Fawzy, A.I. Osman, C. Farrell, A.a.H. Al-Muhtaseb, J. Harrison, A.S. Al-Fatesh, A.H. Fakeeha, J. Doran, H. Yang and D.W. Rooney, *Energy Science & Engineering*, n/a, (2021).
[19] A.I. Osman, T.J. Young, C. Farrell, J. Harrison, A.a.H. Al-Muhtaseb and D.W. Rooney, *ACS Sustainable Chemistry & Engineering*, (2020).
[20] A.I. Osman, A. Abdelkader, C.R. Johnston, K. Morgan and D.W. Rooney, *Industrial & Engineering Chemistry Research*, 56, (2017) 12119.
[21] C. Farrell, A.I. Osman, J. Harrison, A. Vennard, A. Murphy, R. Doherty, M. Russell, V. Kumaravel, A.a.H. Al-Muhtaseb, X. Zhang, J.K. Abu-Dahrieh and D.W. Rooney, *Industrial & Engineering Chemistry Research*, (2021).
[22] C. Jia, J. Chen, J. Liang, S. Song, K. Liu, A. Jiang and Q. Wang, *Journal of Thermal Analysis and Calorimetry*, 139, (2020) 577.
[23] A.I. Osman, A. Abdelkader, C. Farrell, D. Rooney and K. Morgan, *Fuel Processing Technology*, 192, (2019) 179.
[24] S. Fawzy, A.I. Osman, C. Farrell, A.a.H. Al-Muhtaseb, J. Harrison, A.S. Al-Fatesh, A.H. Fakeeha and D.W. Rooney, *Applications in Energy and Combustion Science*, 9, (2022) 100048.
[25] J. Dai and K.J. Whitty, *Fuel*, 263, (2020) 116780.
[26] J. Dai and K.J. Whitty, *Fuel*, 241, (2019) 1214.
[27] J. Dai, L. Hughey and K.J. Whitty, *Fuel Processing Technology*, 201, (2020) 106358.
[28] J. Dai and K. Whitty, *Energy & Fuels*, 32, (2018) 11656.
[29] X. Gao, Y. Zhang, B. Li, Y. Zhao and B. Jiang, *Bioresour Technol*, 218, (2016) 1073.
[30] X. Gao, Y. Zhang, B. Li and X. Yu, *Energy Conversion and Management*, 108, (2016) 120.
[31] A. Ferrer, C. Alciaturi, A. Faneite and J. Ríos, in, 2016, p. 45.
[32] M.A. Herrera, A.P. Mathew and K. Oksman, *Materials Letters*, 71, (2012) 28.
[33] A. Thygesen, J. Oddershede, H. Lilholt, A.B. Thomsen and K. Ståhl, *Cellulose*, 12, (2005) 563.
[34] T. Theivasanthi, F.L. Anne Christma, A.J. Toyin, S.C.B. Gopinath and R. Ravichandran, *Int J Biol Macromol*, 109, (2018) 832.
[35] C. Trilokesh and K.B. Uppuluri, *Sci Rep*, 9, (2019) 16709.
[36] C. Salas, T. Nypelö, C. Rodriguez-Abreu, C. Carrillo and O.J. Rojas, *Current Opinion in Colloid & Interface Science*, 19, (2014) 383.
[37] D. Zheng, Y. Zhang, Y. Guo and J. Yue, *Polymers (Basel)*, 11, (2019) 1130.
[38] N. Kasiri and M. Fathi, *Int J Biol Macromol*, 106, (2018) 1023.
[39] W. Qing, Y. Wang, Y. Wang, D. Zhao, X. Liu and J. Zhu, *Applied Surface Science*, 366, (2016) 404.
[40] A.I. Osman, E. O'Connor, G. McSpadden, J.K. Abu-Dahrieh, C. Farrell, A.a.H. Al-Muhtaseb, J. Harrison and D.W. Rooney, *Journal of Chemical Technology & Biotechnology*, 95, (2019) 183.
[41] C.L. Chiang and J.M. Yang, in D.-Y. Wang (Ed.), *Novel Fire Retardant Polymers and Composite Materials*, Woodhead Publishing, 2017, p. 295.

[42] P.D. Muley, C. Henkel, K.K. Abdollahi, C. Marculescu and D. Boldor, *Energy Conversion and Management*, 117, (2016) 273.
[43] M. Diakite, A. Paul, C. Jager, J. Pielert and J. Mumme, *Bioresour Technol*, 150, (2013) 98.
[44] S. Vyazovkin, K. Chrissafis, M.L. Di Lorenzo, N. Koga, M. Pijolat, B. Roduit, N. Sbirrazzuoli and J.J. Suñol, *Thermochimica Acta*, 590, (2014) 1.
[45] L. Yeng, M.U. Wahit and N. Othman, *Jurnal Teknologi*, 75, (2015).
[46] G.F. Leal, L.A. Ramos, D.H. Barrett, A.A.S. Curvelo and C.B. Rodella, *Thermochimica Acta*, 616, (2015) 9.